

Searching for Stoponium along with the Higgs boson

Vernon Barger*

Department of Physics, University of Wisconsin, Madison, WI 53706

Muneyuki Ishida[†]

*Department of Physics, School of Science and Engineering,
Meisei University, Hino, Tokyo 191-8506, Japan*

Wai.-Yee Keung[‡]

Department of Physics, University of Illinois, Chicago, IL 60680, USA

(Dated: December 17, 2018)

Abstract

Stoponium, a bound state of top squark and its antiparticle in a supersymmetric model, may be found in the ongoing Higgs searches at the LHC. Its WW and ZZ detection ratios relative to the Standard Model Higgs boson can be more than unity from WW^* threshold to the two Higgs threshold. The $\gamma\gamma$ channel is equally promising. A stoponium mass 135 to 150 GeV is severely constrained by the ATLAS and CMS experiments.

Discovery of a Higgs boson h^0 is a top priority of LHC experiments, as is the search for the supersymmetry which is an attractive candidate for physics beyond the SM. Here we make the observation that there is a possibility of finding supersymmetry in the LHC search for the Higgs boson.

The stop \tilde{t}_1 , a scalar superpartner of the top quark, is expected to have the lightest mass of all the squarks[1], and may plausibly be lighter than the top quark. If the mass difference between \tilde{t}_1 and the LSP neutralino \tilde{N}_1 is small and the tree-level decays, $\tilde{t}_1 \rightarrow t \tilde{N}_1$ and $\tilde{t}_1 \rightarrow b \tilde{C}_1$ (where \tilde{C}_1 is the lightest chargino), are not kinematically allowed, the \tilde{t}_1 becomes long-lived and $\tilde{t}_1^* \tilde{t}_1$ will form a bound state called stoponium. This expectation is supported by the result[2] that the partial width of $\tilde{t}_1 \rightarrow c \tilde{N}_1$ occurring at loop level is negligibly small compared with the binding energy of the stoponium, a few GeV.

The possibility of stoponium discovery at hadron colliders was considered long ago[3, 4]. Its production via gg -fusion and its decays are quite similar to the heavy quarkonium of the fourth generation quarks[5]. The production amplitude is proportional to the wave function at the origin, and so the S -wave $J^{PC} = 0^{++}$ bound state, denoted here as $\tilde{\sigma}$, is expected to have the largest production cross section.

Detection of stoponium is complementary to the detection of stop. Actually current LHC data already give a strong limit on the light stop mass[6] by considering the possible decay channels of $\tilde{t}_L \rightarrow \tilde{b}_L W^*$ and $\tilde{t}_L \rightarrow t \tilde{N}_1$. For the parameter space where these decay modes are kinematically forbidden and stop is long-lived, as required for stoponium existence, this constraint does not apply. The stop decays to charm quark and LSP neutralino at loop-level, and this decay mode is notoriously difficult to be identified, because of hadronic effects and the small phase space. In this parameter region, stoponium detection may be the best way to search for supersymmetry.

In this Letter we refine the calculation of the production and decays of the $\tilde{\sigma}$ appropriate to the LHC experiments at 7 TeV (LHC7) and consider the possibility of finding the $\tilde{\sigma}$ in the ongoing LHC Higgs searches. Related work can be found in ref.[7], and more recently in ref.[8], at tree level, and the NLO radiative corrections are considered in refs.[9, 10]. We demonstrate that $\tilde{\sigma}$ could be found in the SM Higgs search in the $\gamma\gamma$ and W^*W^* channels at LHC7. Stoponium can be distinguished from a Higgs boson by differences in decay branching fractions.

Stoponium Production Cross Section

The production cross section of stoponium $\tilde{\sigma}$ in hadron colliders is mainly via gg fusion, similarly to the production of a Higgs boson h^0 . The cross sections are proportional to the respective partial decay widths to gg . The production cross section of h^0 has been calculated in NNLO[11], and by using this result[20] we can directly estimate the production cross section of $\tilde{\sigma}$ as

$$\sigma(pp \rightarrow \tilde{\sigma} X) = \sigma(pp \rightarrow h^0 X) \times \frac{\Gamma(\tilde{\sigma} \rightarrow gg)}{\Gamma(h^0 \rightarrow gg)}. \quad (1)$$

By using the $\Gamma(\tilde{\sigma} \rightarrow gg)$ partial width given later and $\Gamma(h^0 \rightarrow gg)$ of the SM we can predict $\sigma(pp \rightarrow \tilde{\sigma} X)$. The result is compared with the SM Higgs production in Fig. 1.

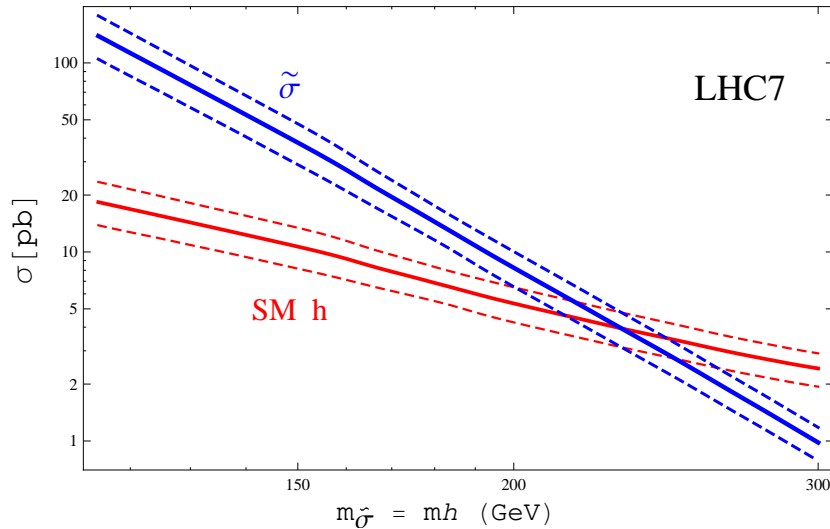


FIG. 1. The production cross section of $\tilde{\sigma}$ [pb] from gg fusion (solid blue), $\sigma(gg \rightarrow \tilde{\sigma})$ [pb], compared with that of the SM Higgs with the same mass $m_{h^0} = m_{\tilde{\sigma}}$ (solid red). The overall theoretical uncertainties[11] are denoted by dotted lines.

The production of $\tilde{\sigma}$ exceeds that of the SM Higgs boson of the same mass $m_{h^0} = m_{\tilde{\sigma}}$ for $m_{\tilde{\sigma}} < 230$ GeV. This is because the $\tilde{\sigma}$ production from gg fusion has an amplitude from the 4-point coupling at tree level, while h^0 production is governed by the one-loop diagram of the top quark. Our prediction of $\sigma(gg \rightarrow \tilde{\sigma})$ in Fig.1 includes the $\pm 25\%$ uncertainty associated with the theoretical uncertainty on $\sigma(gg \rightarrow h^0)$.

Stoponium Decay For the $\tilde{\sigma}$ decay channels $\tilde{\sigma} \rightarrow AB$, we consider $AB = gg, \gamma\gamma, Z\gamma, W^+W^-$,

$ZZ, b\bar{b}, t\bar{t}$, and h^0h^0 . Their partial widths are given by the formula

$$\Gamma(\tilde{\sigma} \rightarrow AB) = \frac{3}{32\pi^2(1 + \delta_{AB})} \frac{2p(m_{\tilde{\sigma}}^2; m_A^2, m_B^2)}{m_{\tilde{\sigma}}} \times \frac{|R(0)|^2}{m_{\tilde{\sigma}}^2} \sum |\mathcal{M}|^2, \quad (2)$$

where \mathcal{M} represent the free $\tilde{t}_1\tilde{t}_1^* \rightarrow AB$ amplitude, p is the momentum of particle A (or B) in the CM system, and $R(0)$ is the radial wave function of stoponium at the origin. The total width $\Gamma_{\tilde{\sigma}}^{\text{tot}}$ is the sum of these partial widths. Here we omit the LSP neutralino channel $AB = \tilde{N}_1\tilde{N}_1$, which is a suppressed decay mode[7, 8]. All the relevant formula are given in the previous works[4, 7, 8], so we briefly explain here our method and the selection of parameters.

In calculations of the amplitude $\mathcal{M} = \mathcal{M}(\tilde{t}_1\tilde{t}_1^* \rightarrow AB)$, the mass of the lighter higgs h^0 is fixed to $m_{h^0} = 125$ GeV, and a maximal-mixing $\theta_{\tilde{t}} = \pi/4$ between the two stops \tilde{t}_L and \tilde{t}_R is taken. The value of $\tan\beta = v_u/v_d$, the ratio of vacuum expectation values of the two Higgs doublets in SUSY, is taken to be 10, and the higgs mixing angle α is also fixed from the tree-level formula, $\tan 2\alpha = [((m_A^2 + M_Z^2)/(m_A^2 - M_Z^2))\tan 2\beta]$, with the choice $m_A = 800$ GeV, for which $\tan\alpha = -0.103$.[21]

The contribution from the heavier higgs H^0 and the heavier stop \tilde{t}_2 to the amplitudes are neglected under the assumption that they are heavy. Amplitudes of t -, u - channel \tilde{t} or \tilde{b} exchanges are neglected except for the \tilde{t}_1 exchange in the h^0h^0 channel. Then, all the amplitudes are described by the contact 4-point interaction and/or the s -channel h^0 amplitudes when they contribute. The Feynman diagrams of our analysis are shown in Fig. 2.

For the gg decay of $\tilde{\sigma}$ we include the radiative corrections at NNLO by using the K-factor from Higgs production[22]. For decay to $\gamma\gamma$ a special attention is taken by ref.[9] since this branching fraction is larger than that of the Higgs boson for which a strong cancellation between top-quark and W loops occurs. We use the $R^{(1)} = \Gamma(\tilde{\sigma} \rightarrow \gamma\gamma)/\Gamma(\tilde{\sigma} \rightarrow \text{hadrons})$ at NLO in Ref.[9], equating their $\Gamma(\tilde{\sigma} \rightarrow \text{hadrons})$ to our $\Gamma(\tilde{\sigma} \rightarrow gg)$. Multiplying $R^{(1)}$ by our $\Gamma(\tilde{\sigma} \rightarrow gg)$, we obtain $\Gamma(\tilde{\sigma} \rightarrow \gamma\gamma)$. The off-shell $WW^*(ZZ^*)$ channels in the low-mass $\tilde{\sigma}$ case are treated following ref.[13].

The gg partial decay width of $\tilde{\sigma}$ is proportional[5] to $(|R(0)|/m_{\tilde{\sigma}})^2$. We use the non-relativistic quark model with the Wisconsin potential, where a potential term in the intermediate range is added to Cornell potential, to obtain the value of $|R(0)|$ [5, 14]. The binding energy, a few GeV, is much smaller than $m_{\tilde{t}_1}$ and the stoponium mass $m_{\tilde{\sigma}}$ is well

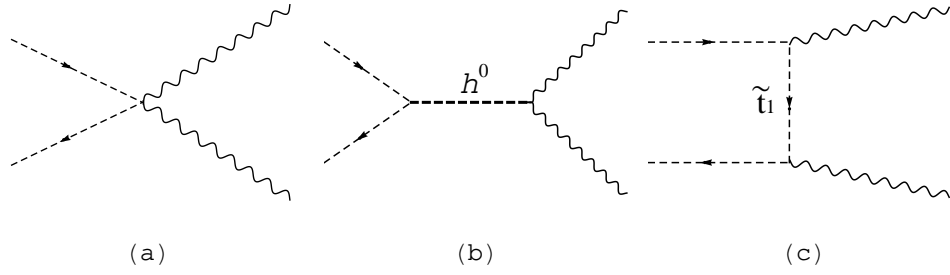


FIG. 2. Dominant generic diagrams of $\tilde{\sigma}$ decay. Thin dashed lines with arrows represent the initial $\tilde{t}_1 \tilde{t}_1^*$ of $\tilde{\sigma}$ and two wavy lines represent the final states $\bar{X}X$. Diagram (a) is taken into account in $\bar{X}X = gg, \gamma\gamma, Z\gamma$, diagram (b) in $\bar{X}X = \bar{b}b$, and diagrams (a) and (b) in $\bar{X}X = WW, ZZ$, while all three diagrams contribute to $\bar{X}X = h^0 h^0$.

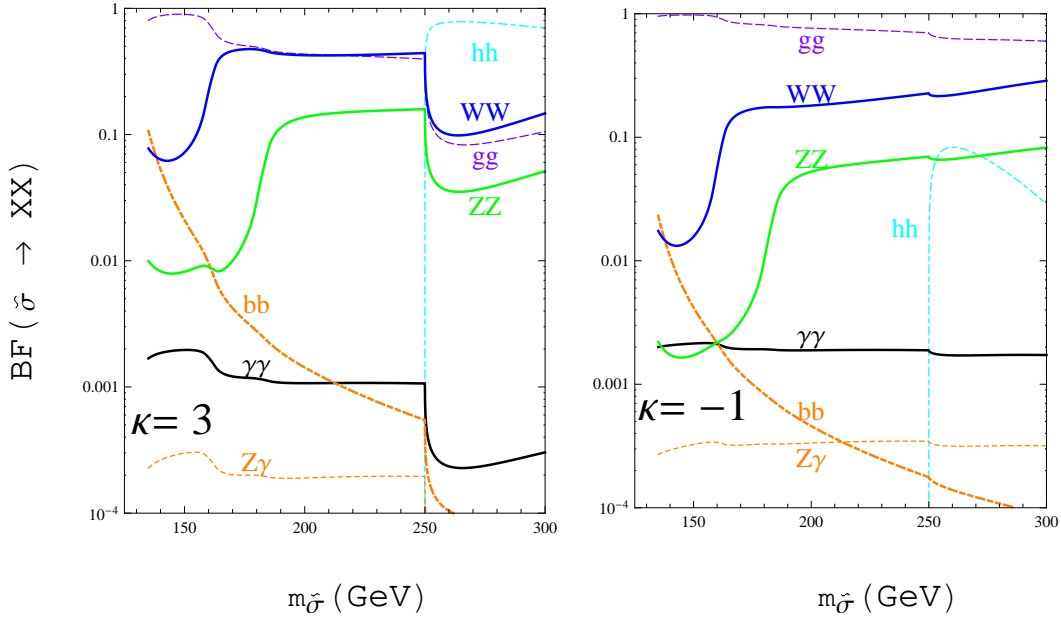


FIG. 3. Decay Branching Fractions of $\tilde{\sigma}$ versus $m_{\tilde{\sigma}}$ (GeV) for $\kappa = 3$ and -1 . m_{h^0} is taken to be 125 GeV.

approximated by $2m_{\tilde{t}_1}$.

With these simplifications, the results depend only upon two quantities, $m_{\tilde{\sigma}}$ and the $h^0 \tilde{t}_1 \tilde{t}_1^*$ coupling $\lambda_{h^0 \tilde{t}_1 \tilde{t}_1^*}$, denoted as $m_{\tilde{t}_1} \lambda_2$ in our previous work[4]. The $\lambda_{h^0 \tilde{t}_1 \tilde{t}_1^*}$ is determined

by a dimensionless parameter κ . [23] In our illustrations we consider two values of κ , $\kappa = 3$ and -1 , which correspond to the strong and weak $h^0\tilde{t}_1\tilde{t}_1^*$ coupling, respectively. The $m_{\tilde{\sigma}}$ is taken as a free parameter varying a wide range, $135 \text{ GeV} < m_{\tilde{\sigma}} < 300 \text{ GeV}$. Below 135 GeV, the mixing between $\tilde{\sigma}$ and h^0 (with m_{h^0} taken to be 125 GeV here) may be important, although this mixing can be handled if necessary.

The decay branching fractions of $\tilde{\sigma}$ are given in Fig. 3. In the case of $\kappa = 3$ [larger $\lambda_{h^0\tilde{t}_1\tilde{t}_1^*}(= 396)$ GeV case], the branching fractions of $WW, ZZ, h^0h^0, b\bar{b}, t\bar{t}$ are larger than those for $\kappa = -1$ [smaller $\lambda_{h^0\tilde{t}_1\tilde{t}_1^*}(= 169)$ GeV case] because of larger contributions from the s -channel h^0 diagram. WW, ZZ, h^0h^0 branching fractions become even larger in the $\kappa = 10$ case, where WW is dominant in $2m_W < m_{\tilde{\sigma}} < 2m_{h^0}$. In the $\kappa = -1$ case, the decay amplitude to h^0h^0 vanishes when $m_{\tilde{\sigma}} \simeq 370 \text{ GeV}$ because of a destructive interference among the 4-point interaction, t, u -channel \tilde{t}_1 exchange and the s -channel h^0 diagrams. The existence of this cancellation has not been previously noted in the literature.

The total width of $\tilde{\sigma}$ in the mass range $m_{\tilde{\sigma}} = 135 \sim 250 \text{ GeV}$ is fairly small, $\Gamma_{\tilde{\sigma}}^{\text{tot}} \sim 2$ to 7 MeV, and in the mass range $m_{\tilde{\sigma}} = 260 \sim 300 \text{ GeV}$, it is at most $\sim 40 \text{ MeV}$ for the $\kappa = 3$ case. Thus a $\tilde{\sigma}$ resonance would be observed with the width of the experimental resolution. At $m_{\tilde{\sigma}} > 2m_W$ the $\Gamma(\tilde{\sigma} \rightarrow WW)$ partial width is negligibly small compared with $\Gamma(h^0 \rightarrow WW)$, and thus $\tilde{\sigma}$ production via vector boson(WW, ZZ) fusion is negligible at the LHC.

The ZZ to WW ratio of the $\tilde{\sigma}$ decay branching fraction is predicted to be $0.32 \sim 0.36$ (for $\kappa = 3$) in the mass range $200 \text{ GeV} < m_{\tilde{\sigma}} < 300 \text{ GeV}$, as compared with $0.36 \sim 0.44$ of the SM h^0 in the same mass range. This ratio can be used to check if an observed resonance is actually stoponium or not.

Stoponium Detection compared to SM Higgs Next we consider the detection of $\tilde{\sigma}$ in W^+W^-, ZZ and $\gamma\gamma$ channels. The $\tilde{\sigma}$ search can be made in conjunction with the Higgs search. The properties of h^0 at the LHC are well known, so we use them as benchmarks of the search for $\tilde{\sigma}$.

The $\tilde{\sigma}$ detection ratio (DR) to h^0 in the $\bar{X}X$ channel is defined[15] by

$$DR \equiv \frac{\Gamma_{\tilde{\sigma} \rightarrow gg} \Gamma_{\tilde{\sigma} \rightarrow \bar{X}X} / \Gamma_{\tilde{\sigma}}^{\text{tot}}}{\Gamma_{h^0 \rightarrow gg} \Gamma_{h^0 \rightarrow \bar{X}X} / \Gamma_{h^0}^{\text{tot}}}, \quad (3)$$

where $\bar{X}X = W^+W^-, ZZ$, and $\gamma\gamma$. The DR are plotted versus $m_{\tilde{\sigma}} = m_{h^0}$ in Fig. 4 for the two cases $\kappa = 3$ and -1 .

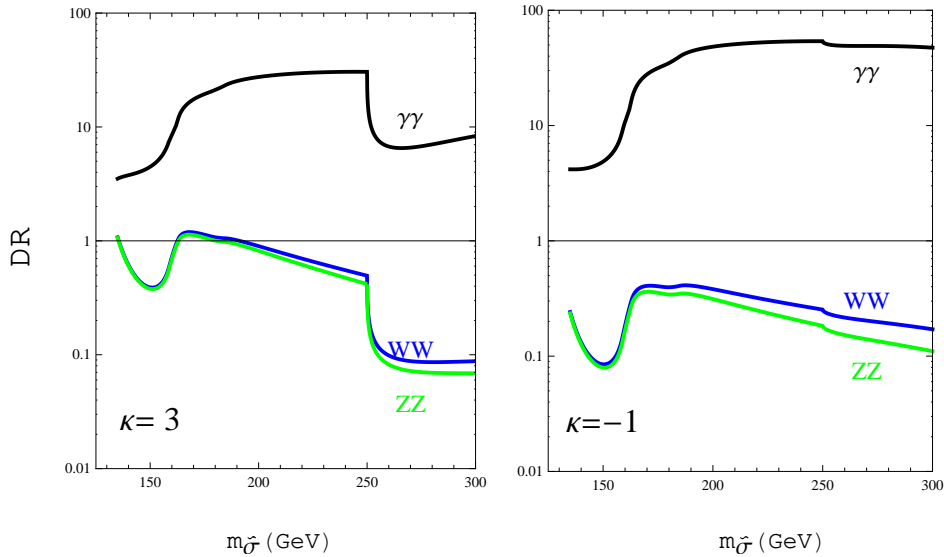


FIG. 4. $\tilde{\sigma}$ Detection Ratio (DR) to the SM higgs h^0 of Eq. (3) for the $\bar{X}X = W^+W^-$ (solid blue), ZZ (dashed green), and $\gamma\gamma$ (solid black) final states for $\kappa = 3, -1$ versus $m_{\tilde{\sigma}}$ (GeV).

In the case of $\kappa = 3$ (the large $\lambda_{h^0\tilde{t}_1\tilde{t}_1^*}$ case), the $\tilde{\sigma}$ to h^0 detection ratio is relatively large in both WW and ZZ channels. The ratio is more than 0.5 in the mass range $160 < m_{\tilde{\sigma}} < 250$ GeV between the WW threshold and the h^0h^0 threshold. For $m_{\tilde{\sigma}} < 190$ GeV the ratio is nearly unity. Even in the $\kappa = -1$ case, the detection ratio is large in the $160 < m_{\tilde{\sigma}} < 250$ GeV mass range.

The cross-section of a putative Higgs-boson signal, relative to the Standard Model cross section, as a function of the assumed Higgs boson mass, is widely used by the experimental groups to determine the allowed and excluded regions of m_{h^0} . By use of the DR in Fig. 4, we can determine the allowed region of $m_{\tilde{\sigma}}$ from the present LHC data. Figure 5 shows the 95% confidence level upper limits on Higgs-like $\tilde{\sigma}$ signals decaying into $\bar{X}X$ versus $m_{\tilde{\sigma}}$ for $\bar{X}X = WW$ and ZZ combined (ATLAS[16][24]) and $\gamma\gamma$ (ATLAS[18]).

For $\kappa = 3$, $m_{\tilde{\sigma}}$ is excluded by ATLAS data over wide ranges of $m_{\tilde{\sigma}}$ 155-227 GeV, while for the $\kappa = -1$ some regions of $m_{\tilde{\sigma}}$ are excluded. Similar results are found from CMS data[17].

The $\tilde{\sigma}$ search is also applicable to the Tevatron data. The CDF and D0 experiments excluded the SM Higgs with mass $158 \text{ GeV} < m_{h^0} < 175 \text{ GeV}$ from the data of WW, ZZ channels. The same data excludes $\tilde{\sigma}$ in the $\kappa = 3$ case in the mass range, $160 \text{ GeV} < m_{\tilde{\sigma}} <$

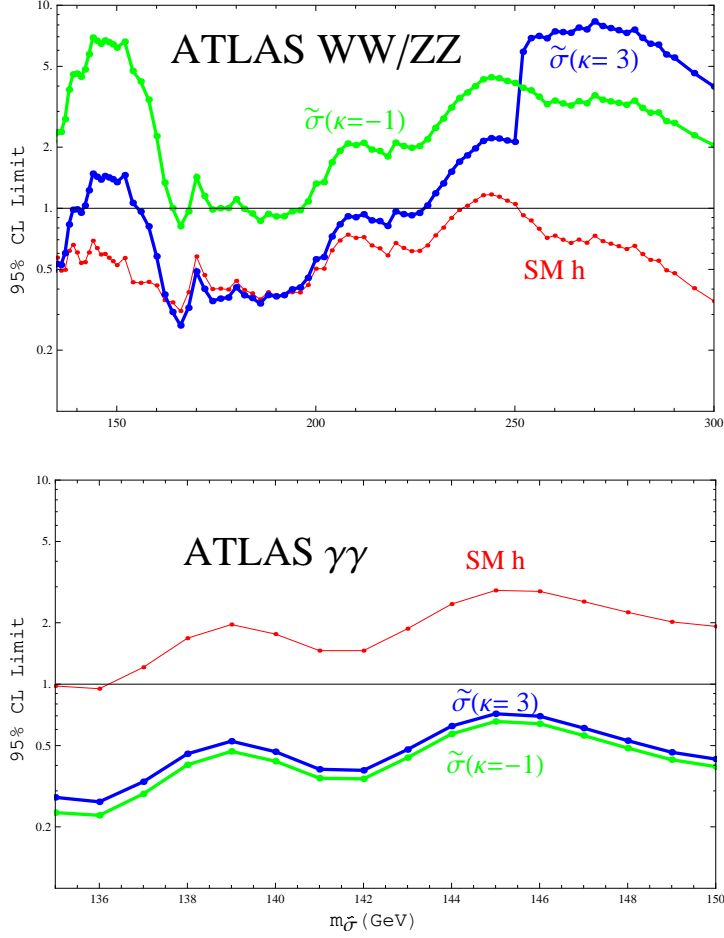


FIG. 5. the 95% confidence level upper limits of $(1/DR) \times (\sigma_{\text{exp}}/\sigma(gg \rightarrow h^0 \rightarrow \bar{X}X))$. This is the signal of a boson decaying into $\bar{X}X$ relative to the stoponium cross section $[\sigma(gg \rightarrow \tilde{\sigma} \rightarrow \bar{X}X) = \sigma(gg \rightarrow h^0 \rightarrow \bar{X}X) \times DR]$ for $\bar{X}X = WW$ (ATLAS[16]) and $\gamma\gamma$ (ATLAS[18]) data. The cases $\kappa = 3$ (solid blue) and -1 (solid green) are shown. Similar results for the SM Higgs boson are also given (red thin-solid curve).

177 GeV.

The $\gamma\gamma$ final state is very promising for $\tilde{\sigma}$ detection, because the $\tilde{\sigma}$ to h^0 detection ratio is generally very large in all the mass range of $m_{\tilde{\sigma}}$, as shown in Fig. 4. From the $\gamma\gamma$ data of ATLAS the region of stoponium mass $135 < m_{\tilde{\sigma}} < 150$ GeV is already excluded in both the cases of κ . The κ -dependence of DR in $\gamma\gamma$ is small below WW threshold because the partial widths of all the allowed two-body final states are independent of κ . For $m_{\tilde{\sigma}} > 150$ GeV, the $\gamma\gamma$ signal of h^0 is too small to be detected, but the data in this region can determine

the existence of $\tilde{\sigma}$.

Concluding Remarks We have investigated the possibility of finding stoponium $\tilde{\sigma}$ at LHC7. In the optimistic case of the stoponium mass and coupling, $\tilde{\sigma}$ will be discovered in the WW , ZZ , and $\gamma\gamma$ channels in the search for the SM Higgs h^0 . The detection rates can be comparable to that of the SM h^0 , in the mass region $m_{\tilde{\sigma}} \sim 160$ GeV up to $2m_{h^0}$ as shown in Fig. 4. The $\gamma\gamma$ search channel is particularly promising since $\tilde{\sigma}$ detection relative to h^0 is very large (more than 3) in all mass regions. A stoponium mass in the 135-150 GeV is already excluded in a wide range of supersymmetry parameters from the present ATLAS $\gamma\gamma$ data. The h^0h^0 decay of $\tilde{\sigma}$ is another possible mode for discovery, especially for large κ .

Acknowledgements

M.I. is very grateful to the members of phenomenology institute of University of Wisconsin-Madison for hospitalities. This work was supported in part by the U.S. Department of Energy under grants No. DE-FG02-95ER40896 and DE-FG02-84ER40173, in part by KAKENHI(2274015, Grant-in-Aid for Young Scientists(B)) and in part by grant as Special Researcher of Meisei University.

* barger@wisc.edu

† Department of Physics, University of Wisconsin-Madison. A visitor until March 2012.;
mishida@wisc.edu

‡ keung@uic.edu

- [1] J. Ellis and S. Rudaz, Phys. Lett. **B128**, 248 (1983).
- [2] K.-i. Hikasa and M. Kobayashi, Phys. Rev. **D36**, 724 (1987).
- [3] M. J. Herrero, A. Mendez, and T. G. Rizzo, Phys. Lett. **B200**, 205 (1988).
- [4] V. Barger and W.-Y. Keung, Phys. Lett. **B211**, 355 (1988).
- [5] V. Barger, E. W. N. Glover, K. Hikasa, W.-Y. Keung, M. G. Olsson, C. J. Suchyta, and X. R. Tata, Phys. Rev. Lett. **57**, 1672 (1986); Phys. Rev. **D35**, 3366 (1987).
- [6] M. Pappucci, J. T. Ruderman, and A. Weiler, arXiv:1110.6926[hep-ph].
- [7] M. Drees and M. M. Nojiri, Phys. Rev. **D49**, 4595 (1994).
- [8] S. P. Martin, Phys. Rev. **D77**, 075002 (2008).
- [9] S. P. Martin and J. E. Younkin, Phys. Rev. **D80**, 035026 (2009).

- [10] J. E. Younkin and S. P. Martin, Phys. Rev. D**81**, 055006 (2010).
- [11] J. Baglio and A. Djouadi, arXiv:1012.0530v3 [hep-ph].
- [12] S. Catani, D. de Florian, M. Grazzini, and P. Nason, JHEP**07**, 028 (2003)
- [13] W.-Y. Keung and W. J. Marciano, Phys. Rev. D**30**, 248 (1984).
- [14] K. Hagiwara, K. Kato, A. D. Martin, and C. K. Ng, Nucl. Phys. B**344**, 1 (1990).
- [15] V. D. Barger and R. J. N. Phillips, "Collider Physics" Updated Edition, Westview press (1991).
- [16] The ATLAS Collaboration, ATLAS-CONF-2011-163 .
- [17] The CMS Collaboration, CMS PAS HIG-11-032 .
- [18] The ATLAS Collaboration, ATLAS-CONF-2011-161 .
- [19] M. Schreck and M. Steinhauser, arXiv:0708:0916v2 [hep-ph].
- [20] In the approximation that the $gg \rightarrow \tilde{\sigma}$ interaction is essentially point-like, the QCD radiative corrections to the tree level $gg \rightarrow h^0$ and $gg \rightarrow \tilde{\sigma}$ should be nearly equal so we can use the tree level result for $\Gamma(\tilde{\sigma} \rightarrow gg)/\Gamma(h^0 \rightarrow gg)$.
- [21] This formula should be applied with a limit $\alpha \rightarrow \beta - \frac{\pi}{2}$ as $m_A \rightarrow \infty$.
- [22] We use central values of K-factor of Higgs production in NNLO given in Fig. 8 of Ref.[12]: For $m_{h^0} = 100 \sim 300$ GeV, $K = 2.0 \sim 2.3$. This value is about 10% larger than the K-factor of Higgs decaying into gg in NNLO given in ref.[19] but within the uncertainty of the choice of the renormalization scale. So we simply assume they are equal and adopt the value in ref.[12] . Here we also note that the K factor for $\tilde{\sigma}$ production is calculated in NLO[10] as $K \simeq 1.4$ in $m_{\tilde{\sigma}} = 200 \sim 600$ GeV, which is, contradictorily with our argument[20], 25% smaller than the value $K \simeq 1.9$ in the NLO calculation for h^0 given in ref.[12].
- [23] $\lambda_{h^0 \tilde{t}_1 \tilde{t}_1^*}$ includes a term proportional to $(-\mu \sin\alpha + m_6 A_t \cos\alpha) \equiv \kappa M_W$, where μ is the Higgsino mass term in the superpotential and $m_6 A_t$ is a soft breaking parameter of the trilinear scalar interaction[4].
- [24] DR for WW and ZZ are almost the same, and so we have applied DR for WW to the ATLAS WW and ZZ combined data.